Tribology and Materials
Vol. x, No. x, 202x, pp. xx-xx

ISSN 2812-9717
https://doi.org/10.46793/tribomat.202x.xxx

Investigation on tribological properties of PETG with integrated PTFE inserts

Andrey VASILEV *, Aitalina OKHLOPKOVA, Afanasy DYAKONOV

North-Eastern Federal University, Yakutsk, Russia
*Corresponding author: gtvap@mail.ru

Keywords
PETG
PTFE
additive manufacturing
tribological properties
coefficient of friction

History
Received: 11-09-2025
Revised: 04-12-2025
Accepted: 14-12-2025

Abstract

The parts and components produced from polyethylene terephthalate glycol (PETG) using additive manufacturing techniques require improvements in tribological properties, which represent a significant scientific and technical challenge. The high coefficient of friction and susceptibility to wear of PETG restrict its use in functional parts that operate under sliding conditions. This study, therefore, proposes coaxially integrating cylindrical polytetrafluoroethylene (PTFE) inserts measuring 3 or 6 mm in diameter into 3D printed PETG structures. PETG samples were fabricated using fused deposition modelling and tested under various normal loads (50 – 150 N) at a sliding velocity of 0.2 m/s to evaluate their tribological properties. The experimental results demonstrated that the PTFE inserts reduced the coefficient of friction by up to 68 % (from 0.57 – 0.64 to 0.18 – 0.24) compared to pristine PETG. Samples with a 6 mm insert exhibited the best performance, with a coefficient of friction ranging from 0.18 to 0.24 and up to 75 % wear reduction. PETG serves as a structurally strong matrix, while the PTFE inserts impart excellent anti-friction properties through transfer-film formation. Thermomechanical analysis verified the stability of the materials in the range from 40 to 80 °C. These results highlight the potential of this hybrid material for creating self-lubricating components such as bearings and guides by combining the mechanical strength of PETG with the superior anti-friction properties of PTFE.

1. Introduction

Additive manufacturing, particularly fused deposition modelling (FDM), has significantly transformed production methods. It offers high flexibility and cost-efficiency, as well as the ability to fabricate parts with complex geometries that cannot be achieved using traditional methods, such as injection moulding or machining [1]. These advantages have expanded the use of 3D printing beyond prototyping to include functional components in fields such as mechanical engineering, medicine and electronics. Recent FDM advancements include novel polymers and optimised printing parameters for improved mechanical and tribological performance [2].

Among FDM materials, polyethylene terephthalate glycol (PETG) occupies a special place thanks to its ideal blend of properties: high mechanical strength, chemical resistance, impact toughness and superior interlayer adhesion [3,4]. These properties make PETG a popular choice for producing functional prototypes, electronic enclosures, medical components and protective equipment, including casings and shields [4]. In recent years, applications of PETG have expanded to include tribological components, such as sliding bearings, gears and dampers, that require low friction and high wear resistance [5]. However, compared to other polymers such as polyamide or polyetheretherketone (PEEK), the tribological properties of FDM-printed PETG remain underexplored [6]. For example, when sliding dry against steel, unfilled FDM-printed PETG exhibits high and unstable friction. Vaught and Polycarpou

[5] measured steady-state coefficients of friction (COF) in the range 0.34 – 0.44. Vertically printed specimens exhibited the highest values, as the layered structure exposed weak interlayer boundaries to shear. Similar anisotropy-related issues and pronounced stick-slip behaviour were later confirmed by Jannet et al. [7] and Jagadeesha et al. [8]. At contact pressures above 1.5 MPa, frictional heating can lead to the surface melting and catastrophic failure of pure PETG parts. This severely limits their use in real load-bearing tribological applications such as plain bearings or linear guides.

To address these limitations, active research is being conducted into modifying PETG using various fillers. For example, incorporating graphene into PETG has been shown to reduce wear rates and stabilise the COF [9]. A similar effect has been achieved by modifying the polymer with 3 wt. % organically modified montmorillonite nanoclay, which has been shown to significantly improve wear resistance, as confirmed by neural network models that predict tribological performance [10]. Besides graphene and organically modified montmorillonite nanoclay, other common solid lubricants and reinforcements have also been successfully employed to reduce the friction and wear of PETG parts, including molybdenum disulfide, short carbon and glass fibres, as well as post-processing techniques such as annealing and the application of thin solid-lubricant coatings [7,11,12]. Other studies highlight the significant influence of printing parameters, such as layer orientation, extrusion temperature and surface quality, on PETG's tribological properties [2,5,9]. In particular, combining FDM printing with post-processing mechanical polishing improves surface roughness and reduces the COF [13].

Among the various fillers used to enhance tribological performance, polytetrafluoroethylene (PTFE) is an effective filler for enhancing the tribological properties of polymers due to its exceptionally low COF (0.05 – 0.10) and stability across a wide temperature range (from –200 to 260 °C) [14]. Studies show that incorporating PTFE into polymer matrices, such as polylactic acid (PLA) or polyamide 12 (PA 12), significantly improves mechanical and tribological performance. For instance, incorporating 2 – 3 wt. % PTFE into PLA increases tensile strength by 21.1 % and elastic modulus by 25.5 %. In PA 12, these improvements are 34.1 % and 41.7 %, respectively [15]. However, the effects of PTFE are not always straightforward: in PEEK, for instance, PTFE reduces mechanical strength and improves wear resistance by forming transfer films on contact surfaces [16]. This effect stems from PTFE's ability to generate thin transfer layers on the counter-body, thereby reducing friction and wear in polymer-steel pairs. An alternative approach, proposed by Lin et al. [17], involves using PTFE as a separate composite element (e.g. a pin) to generate lubricating films in the contact zone. This method has been shown to be highly effective in reducing the COF and wear in PEEK-steel pairs, confirming PTFE's potential for tribological applications.

Conventional polymer modification methods using fillers typically involve creating composite blends where the filler is dispersed throughout the entire volume of the material, which can lead to a decline in mechanical strength [17]. Unlike these methods, the present work proposes a macroscopic structural integration (secondary press-fit assembly) approach: solid PTFE cylinders are manufactured separately and press-fitted into 3D printed PETG parts. This simple technique preserves the full mechanical strength of the PETG matrix while providing localised low-friction zones. This work's practical aims are to coaxially integrate PTFE inserts into PETG matrices, enabling the production of complex geometries with tailored tribological properties. The research investigates the tribological and mechanical properties of PETG/PTFE under varying loads by analysing their thermal stability. The findings have practical applications in the creation of sliding bearings, guide systems and other tribological pairs operating under boundary lubrication. This study expands the potential of PETG in additive manufacturing by facilitating the development of efficient, self-lubricating components.

2. Experimental

2.1 Materials

Black PETG filament Geeetech PETG (HK Getech Co., China), 1.75 mm in diameter, was dried at 50 °C for 4 hours to remove moisture and prevent extrusion defects. The density of PETG was 1.27 g/cm^3, with a melting point in the range of approximately 220 – 260 °C. PTFE powder PN-90 (HaloPolymer, Russia) was used for the inserts. The powder had an average particle size of approximately 90 µm, a density of 2.16 g/cm^3 and a melting point of 327 ± 5 °C.

2.2 Fabrication process

PTFE inserts were fabricated by compacting the powder at 50 MPa using a hydraulic press, followed by sintering at 375 ± 5 °C for 2 hours in a programmable furnace. Cylindrical PETG samples (10 mm diameter, 20 mm height) were fabricated via FDM on a Creality Ender-3 S1 Pro 3D printer. A central cylindrical hole (3 or 6 mm diameter, 5 mm depth, ± 0.05 mm tolerance) was incorporated into each sample during the CAD design stage. G-code was generated using UltiMaker Cura 5.5. The optimised printing parameters are listed in Table 1.

Table 1. Optimised FDM printing parameters for PETG samples

Parameter	Value
Nozzle temperature, °C	230
Bed temperature, °C	70
Nozzle diameter, mm	0.4
Printing speed, mm/s	60
Layer height, mm	0.2
Infill density, %	100
Infill orientation, °	linear ±45 pattern
Wall thickness, mm	0.4 (2 walls)

Cylindrical PTFE inserts (3 or 6 mm diameter, 8 – 9 mm height) were press-fitted into the holes immediately after printing and trimmed flush with the PETG surface. No additional surface finishing (polishing or annealing) was applied, so all PETG samples were tested in their as-printed condition. The excess PTFE was then trimmed to create a smooth contact surface. A press-fit creates significant mechanical stress at the interface, ensuring a reliable bond between the PETG and PTFE and preventing the insert from dislodging under operational loads. The geometry and arrangement of the inserts (PETG/PTFE-3 and PETG/PTFE-6, providing approximately 9 % and 36 % PTFE coverage of the nominal contact area, respectively) are shown in Figure 1.

Figures 1a, 1b and 1c illustrate the sample dimensions with cross-sectional schematics, alongside views from the slicing software (UltiMaker Cura). In the cross-sectional views, the hatching on the PETG matrix represents the internal portion into which the corresponding PTFE insert (3 mm or 6 mm) is integrated. The optical micrographs (e.g. the surface view in Fig. 1a and the insert surface in Fig. 1b) were captured at 150× magnification. These micrographs reveal the surface morphology of the as-printed PETG, where individual extruded filaments are visible, as well as the microstructure of the sintered PTFE surface.

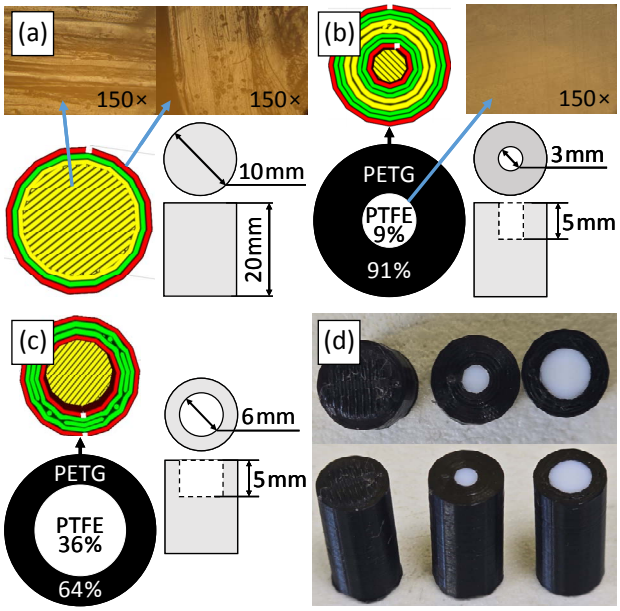

Figure 1. Tested samples: (a) PETG, (b) PETG/PTFE-3, (c) PETG/PTFE-6 and (d) photographs of the samples

2.3 Characterisation

Compression tests of PETG and PTFE samples were conducted on a Shimadzu AGS-J universal testing machine, in accordance with ISO 604. Tests were performed on cylindrical specimens (10 mm diameter, 20 mm height) at a deformation rate of 1 mm/min and ambient temperature of 23 ± 1 °C. The measured parameters included compressive stress at 5 % strain in MPa and compressive modulus in MPa. Five specimens were tested for each material. Hardness measurements were carried out using a Vostok-7 TBP-D durometer on the Shore D scale, in accordance with ISO 868. Tests were conducted at 23 ± 1 °C, with five specimens evaluated per material.

Material density was determined via hydrostatic weighing according to GOST 15139-69, using distilled water at 23 ± 1 °C. Three specimens were tested for each material. The coefficient of thermal expansion was measured using a Shimadzu TMA-60 thermomechanical analyser, in accordance with ISO 11359-2. The mean coefficient of linear thermal expansion (CLTE) was measured on 10 × 5 mm specimens under a 4 kPa load (approximately 3 g) across a temperature range of 40 – 200 °C at a heating rate of 5 °C/min.

Tribological tests were performed on a Bruker UMT-3 tribometer using a pin-on-disc configuration. The tribometer is equipped with a

high-rigidity frame and active vibration isolation, and specimens were rigidly fixed in a dedicated holder to eliminate measurable vibrations and stick-slip after the initial run-in period. The test parameters were as follows: rotational speed of 96 rpm (sliding speed of 0.2 m/s), normal loads of 50, 100, and 150 N (corresponding to contact pressures of 0.64, 1.27, and 1.91 MPa, respectively) and a test duration of 1 hour. The counter-body was a steel C45 disc with a hardness of 45 – 50 HRC and a surface roughness of *Ra* = 0.06 – 0.08 µm. Specimens were cylindrical (10 mm diameter, 20 mm height), with three samples tested per material. The coefficient of friction was continuously recorded and averaged after reaching steady-state at 200 m. Specimen mass was measured using analytical balances before and after testing.

Surface temperature was additionally recorded using an IRay Technology IX2 thermal imaging camera (measurement accuracy ±3 °C). Worn surfaces were examined using an Olympus BX41 optical microscope. Fourier-transform infrared (FTIR) spectroscopy was conducted using a Varian 7000 FTIR spectrometer with an attenuated total reflection accessory, covering the 550 – 4000 cm^{-1} range. This method enabled the investigation of changes in the chemical structure of the surface before and after tribological testing. Images of the sample surfaces were obtained using a JEOL JSM-7800F scanning electron microscope with an Oxford Instruments energy-dispersive X-ray spectroscopy (EDS) attachment.

3. Results and discussion

The mechanical properties and density of the pristine PETG and PTFE materials used in this study are summarised in Table 2. According to Table 2, PETG exhibits significantly higher compressive mechanical properties than PTFE. At 5 % strain, PETG's strength of 35 MPa is 3.5 times greater than that of PTFE's strength of 10 MPa, while PETG's modulus of elasticity is 2.9 times higher. This substantial difference arises from the distinct molecular structures of the materials. PETG, being a polyester, is more rigid and provides superior resistance to compressive deformation compared to the compliant and softer fluoropolymer PTFE.

PETG also demonstrates significantly higher Shore D hardness (76 ± 1) than PTFE (56 ± 1). These values are similar to the Shore D range of 73 – 78 reported by Guessasma et al. (2019) [18] and Jannet et al. [7] for FDM-printed PETG. The compressive strength of 32 MPa at 5 % strain obtained by Jannet et al. [7] for annealed specimens and the typical Shore D value of 53 – 58 documented for sintered PTFE by Struchkova et al. [14] confirm that both materials in our study retain the standard mechanical characteristics representative of their respective classes. The density of pristine PTFE (2.16 ± 0.01 g/cm^3) is 1.7 times higher than that of PETG (1.26 ± 0.02 g/cm^3), which is consistent with the literature values of 1.27 g/cm^3 for PETG [18] and 2.16 g/cm^3 for PTFE [14]. This density difference must be considered when designing lightweight structures where mass is critical.

Table 2. Mechanical properties and density of pristine PETG and PTFE

Characteristic	PETG	PTFE
Compressive stress at 5 % strain, MPa	35 ± 2	10 ± 1
Compressive modulus of elasticity, MPa	766 ± 40	261 ± 40
Shore D hardness	76 ± 1	56 ± 1
Density, g/cm^3	1.26 ± 0.02	2.16 ± 0.01

The noticed differences in mechanical and physical characteristics stem from the polymers' distinct molecular structures. These results confirm that, as a stiffer and harder material, PETG is better suited to structural applications, while PTFE retains its advantages despite its lower mechanical characteristics due to its superior anti-friction properties.

The thermomechanical analysis (TMA) results for the PETG and PTFE samples are presented in Table 3 and Figure 2. The TMA revealed distinct differences in the behaviour of PTFE and PETG when heated. PTFE exhibits complex temperature-dependent behaviour. In the 40 – 70 °C range, it shows moderate expansion with a CLTE of 115×10^{-6} – 163×10^{-6} 1/K. This is followed by stabilisation at 80 – 100 °C, with a subsequent decrease in CLTE to approximately 137×10^{-6} 1/K at temperatures above 100 °C. This behaviour is associated with the rearrangement of the material's crystalline structure and is characteristic of high-temperature polymers. PTFE is known to maintain stable operational properties over a wide temperature range of 25 – 260 °C [19].

Table 3. Comparison of CLTE of PETG and PTFE

Temperature, °C	CLTE × 10^{-6}, 1/K	
	PETG	PTFE
40 – 50	49.30	115.38
50 – 60	54.67	119.71
60 – 70	65.61	153.37
70 – 80	116.90	163.46
80 – 90	159.24	153.85
90 – 100	567.79	144.71
100 – 110	1833.20	126.44
110 – 120	1874.75	137.02

In contrast, PETG exhibits behaviour that is typical of amorphous polymers. Within the temperature range of 75 – 85 °C, a sharp increase in CLTE is noticed, rising from 50 – 150 × 10^{-6} to 568 – 1875 × 10^{-6} 1/K, which indicates a transition to a highly elastic state [4,20]. Below its glass transition temperature, PETG demonstrates a low CLTE and stable dimensions, which are characteristic of the glassy state.

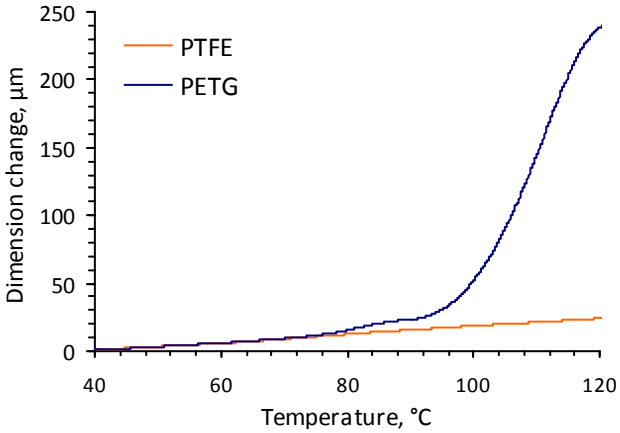

Figure 2. TMA curves of PTFE and PETG samples

As shown in Figure 2, despite differences in CLTE values, the dimensional changes in the TMA curves from 40 to 80 °C are almost identical for both polymers. Therefore, the PTFE/PETG material can perform optimally within the temperature range from room temperature to 80 °C. This should be taken into account when using products based on these materials.

Figure 3 shows typical coefficient of friction (COF) curves for the entire testing period of the specimens under a normal load of 100 N, where 3 and 6 refer to the insert size in millimetres. As shown in Figure 3, the PETG/PTFE-6 sample exhibits a smoother and more stable COF curve from the beginning of the test. In contrast, PETG/PTFE-3 shows an initial increase in COF under a 100 N normal load during the run-in period before stabilising.

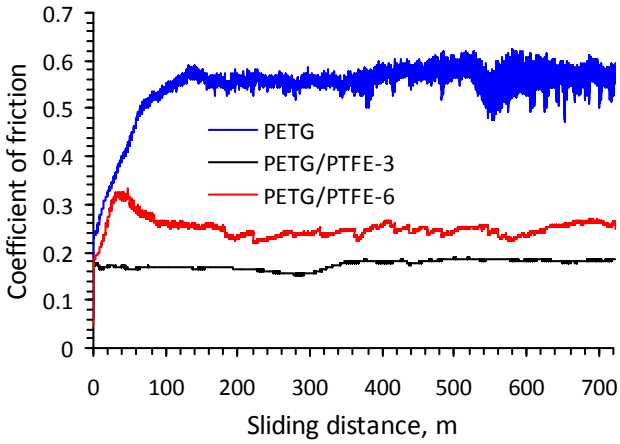

Figure 3. Coefficient of friction curves under a normal load of 100 N

Figure 4 shows the COF and mass loss results for PETG, as well as for the combined PETG/PTFE-3 and PETG/PTFE-6 materials. It should be noted that the COF was taken for the steady-state period. As shown in Figure 4, pristine PETG exhibits a high COF, ranging from 0.58 to 0.64 under normal loads of 50 – 150 N. Similar results were reported by Jagadeesha et al. [8], who found that PETG exhibited a COF of 0.5 under dry sliding conditions. The integrated PTFE insert in PETG significantly reduces the COF. For PETG/PTFE-3, the COF in steady-state ranged from 0.20 to 0.30 depending on normal load, which corresponds to a reduction of 53 – 66% compared to pristine PETG. The PETG/PTFE-6 showed even lower values of 0.18 – 0.24, representing a maximum reduction of up to 69 % compared to pure PETG.

This reduction in COF is attributed to the self-lubricating properties of PTFE, which form a thin lubricating film on the material's surface [21]. The lower COF and markedly improved wear resistance of PETG/PTFE-6 compared to PETG/PTFE-3 are attributed to the significantly larger PTFE contact area (36 % versus 9 % of the total nominal surface area). Although Amonton's law states that friction is independent of apparent contact area, in dry sliding polymer-metal contacts, the real contact area is load-dependent and governed by viscoelastic/plastic deformation of the softer phase. The fourfold higher fraction of low-shear-strength PTFE in the real contact zone of PETG/PTFE-6 directly reduces frictional resistance despite identical nominal contact area (approximately 78.5 mm^2) of all specimens.

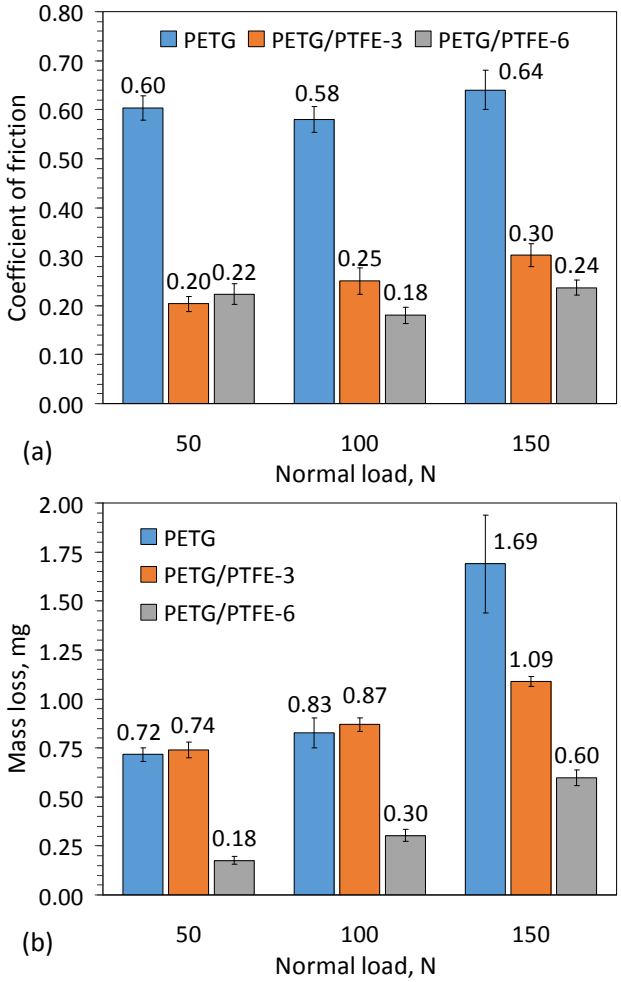

Figure 4. Tribological properties of PETG and PETG/PTFE samples as a function of normal load: (a) coefficient of friction and (b) mass loss

In this study, mass loss is used as an indicator of the material's wear resistance. For pristine PETG, mass loss increases with load. Under 50 N, the mass loss was 0.72 mg and under 100 N, it was 0.83 mg. Under a normal load of 150 N, the pristine PETG underwent geometric change in shape due to heat generated by friction, which caused surface melting of the polymer followed by material displacement, as also reported by Jannet et al. [7] and Jagadeesha et al. [8]. The average mass loss for this sample was 1.69 mg, and the COF was 0.64. Although the COF of PETG/PTFE-3 was markedly lower, its mass loss remained comparable to that of pristine PETG. This can be explained by the limited PTFE coverage of only 9 % of the contact surface, which was insufficient to form a continuous transfer film. As a result, the surrounding PETG continued to experience abrasive wear, while the small insert itself was subjected to higher local pressures, accelerating its degradation. In contrast, the PETG/PTFE-6 sample demonstrates a significant reduction in wear, with mass loss of 0.18 mg under 50 N, 0.30 mg under 100 N and 0.60 mg under 150 N, representing reductions of up to 76 % compared to pristine PETG and PETG/PTFE-3 at the same loads.

Under a normal load of 50 N, the COF difference between PETG/PTFE-3 and PETG/PTFE-6 is negligible. A notable divergence emerges at higher loads (100 and 150 N), where the COF increases for all materials, likely due to elevated contact stresses and frictional heating [22]. Thus, heat generation due to friction is most critical at the maximum applied load of 150 N (corresponding to 1.91 MPa), at which pristine PETG exhibited shape deformation and the highest risk of thermal softening. Therefore, the surface temperature was monitored with a thermal imaging camera only under these most severe sliding conditions. Measurements were taken at the beginning (during the first minute), in the middle (between the 29th and 30th minutes) and at the end (after 59 minutes) of the one-hour test. The results are presented in Table 4.

Table 4. Table 4. Surface temperature of the samples during tribological testing under a normal load of 150 N

Sample	Temperature, °C		
	initial	mid-test	end
PETG	25.4	50.4	60.9
PETG/PTFE-3	26.0	44.0	45.9
PETG/PTFE-6	25.5	38.7	39.3

The highest surface temperature recorded during the 150 N tests was 60.9 °C for pristine PETG and below 46 °C for both hybrid materials (Table 4). These values are substantially lower than the glass transition temperature of PETG (80 – 85 °C). Therefore, the catastrophic wear and macroscopic shape deformation noticed only on pristine PETG under 150 N cannot be attributed to bulk thermal softening or surface melting of the polymer. Instead, they result primarily from high contact stresses (about 1.91 MPa nominal, locally much higher due to surface asperities) combined with strong adhesive transfer and abrasive ploughing typical of unfilled PETG sliding against steel [5,7,8]. In contrast, the significantly lower temperatures at the PETG/PTFE hybrids directly reflect the formation of a thin, low-shear-strength PTFE transfer film that dramatically reduces both friction force and localised flash heating. This confirms that the PTFE inserts effectively suppress the mechanisms responsible for the failure of pristine PETG under the same severe loading conditions.

Although adding PTFE powder to polymers is a common method for reducing friction, no direct comparison with bulk PETG/PTFE composites was made in this study. Literature data indicate that adding PTFE to plastics for FDM printing usually reduces COF and wear [15,17]. As shown in the study by Samyn and Schoukens [23], larger real contact areas and geometries that retain PTFE wear particles in the contact zone can significantly reduce both friction and wear compared to small contact areas. The 6-millimetre PTFE insert used here (covering 36 % of the area) is likely to create similar favourable conditions.

Figure 5 shows SEM images and the results of EDS analysis of the worn surface of PETG, PETG/PTFE-3 and PETG/PTFE-6 under a normal load of 100 N. As shown in Figure 5a, significant smoothing of the PETG contact surface was noticed after tribological testing. No fibres associated with the FDM manufacturing process of this material were detected. The proposed wear mechanism for pristine PETG involved the abrasive wear of protruding fibres, followed by smoothing. Similar results for PETG were reported by Mathew et al. [13], who also noticed surface smoothing.

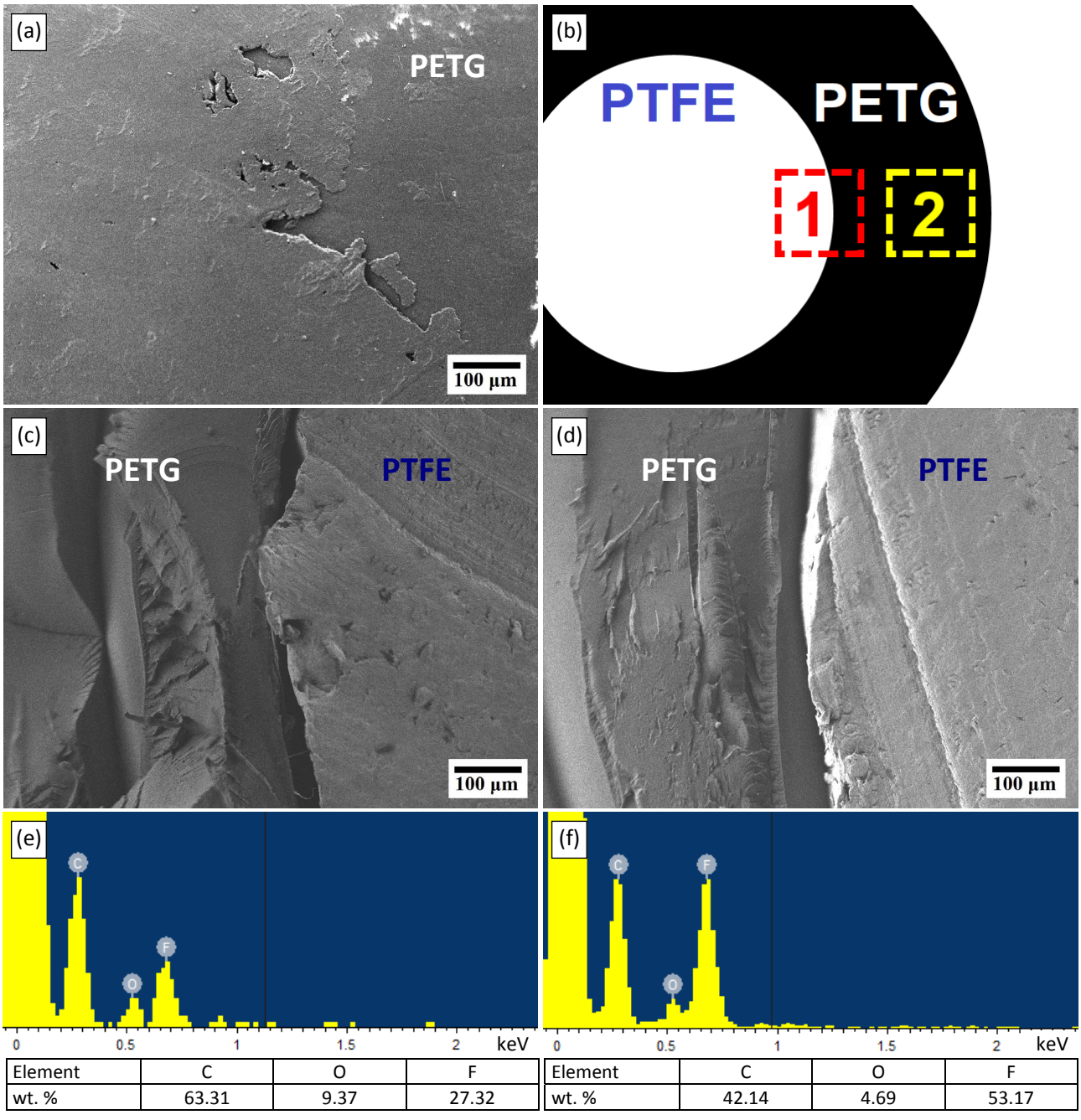

Element	C	O	F
wt. %	63.31	9.37	27.32

Element	C	O	F
wt. %	42.14	4.69	53.17

Figure 5. Worn surface analysis: (a) SEM image of PETG, (b) location for SEM and EDS analysis on PETG/PTFE samples, (c) SEM image of PETG/PTFE-3, (d) SEM image of PETG/PTFE-6, (e) EDS analysis of PETG/PTFE-3 and (f) EDS analysis of PETG/PTFE-6

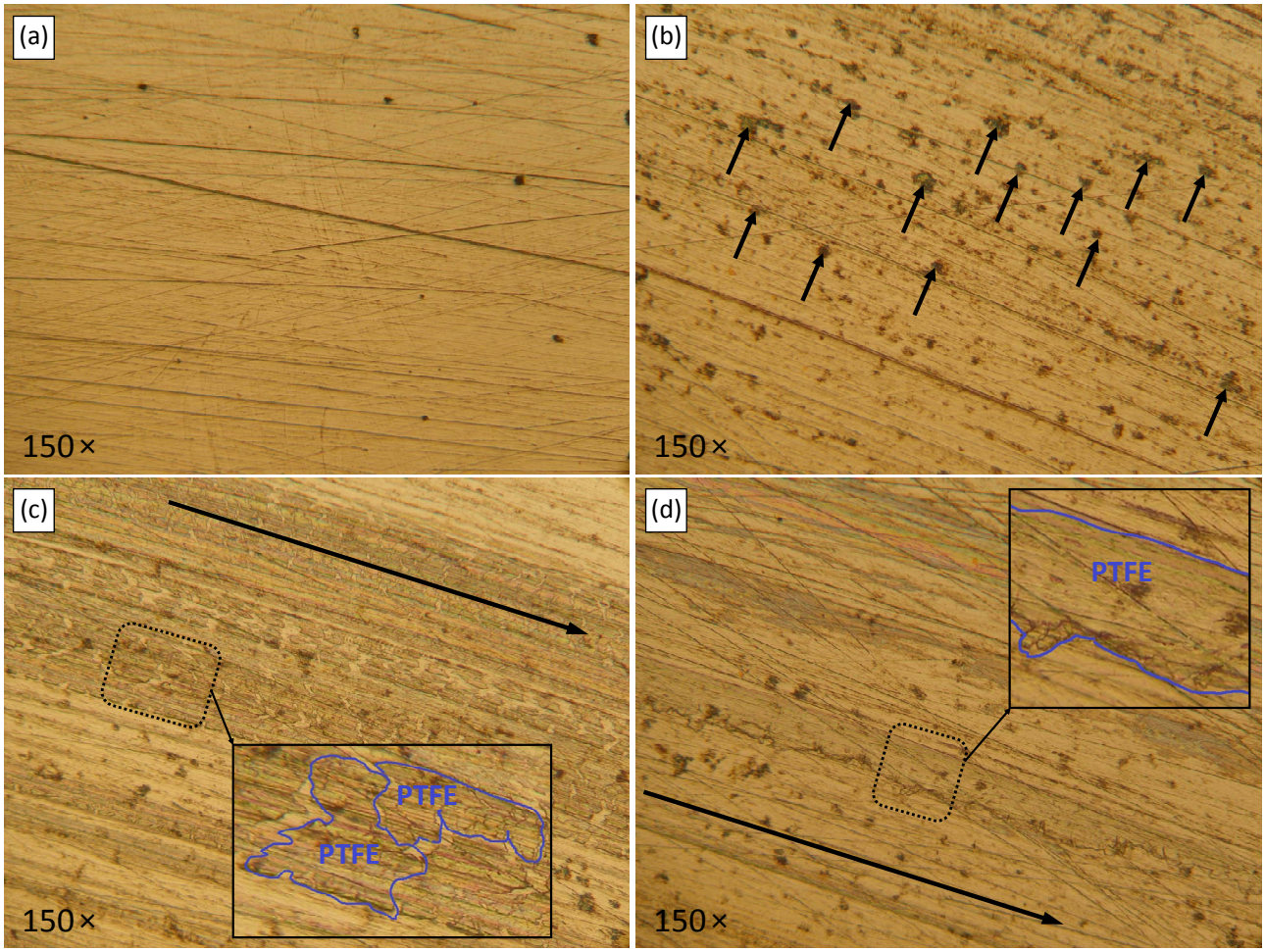

Figure 6. Optical micrographs of the counter-body surface: (a) before testing, (b) after contact with PETG, (c) after contact with PETG/PTFE-3 and (d) after contact with PETG/PTFE-6

SEM images were taken at two locations, as shown in Figure 5b: (1) indicates the boundary between the materials and (2) shows the area for EDS analysis of the PETG surface to indicate the presence of transferred PTFE. No significant gaps were found between the PETG and PTFE at the material boundaries in both the PETG/PTFE-3 and the PETG/PTFE-6 samples. However, the possibility of micro-movement at the interface under prolonged loading cannot be entirely excluded, which may affect long-term stability. Grooves are visible in the PTFE material, which are caused by contact with the steel counter-body. EDS analysis revealed wear products associated with PTFE that remained on the PETG surface between the fibre protrusions in both cases. This reduces the COF of PETG with integrated PTFE inserts.

Figure 6 shows optical micrographs of the counter-body surface before and after the completion of tribological tests under a normal load of 100 N with PETG, PETG/PTFE-3 and PETG/PTFE-6 samples.

Optical microscopy was used to examine the transfer film formed on the counter-body. Analysis of the micrographs after tests with unmodified PETG (Fig. 6b) revealed pinpoint traces of polymer transfer (indicated by arrows), which is characteristic of adhesive wear. For the PETG/PTFE-3 sample (Fig. 6c), a discrete PTFE transfer film formed in the direction of sliding was noticed (highlighted area). This induced a limited reduction in wear, as the PETG matrix still sustained a portion of the contact. In contrast, the PETG/PTFE-6 sample (Fig. 6d) developed a continuous PTFE transfer film in the sliding direction (highlighted area). Only minor traces of PETG were detected on the surface. These results support the previously proposed mechanisms for reducing the COF and minimising wear in PETG/PTFE-6.

Infrared spectroscopic studies of the contact surfaces were conducted on pristine PETG, pristine PTFE and hybrid materials after testing under varying normal loads. Figure 7 shows the results of studying the pristine PETG and PTFE materials before testing. For PTFE, two intense peaks were identified in the region of 1200 and 1145 cm^{-1}, which are related to valence vibrations of C–F

bonds in CF_2 groups. There is also a peak at 639 cm^{-1}, which corresponds to deformation vibrations of CF_2.

The FTIR spectrum of pristine PETG shows characteristic peaks corresponding to the polymer's main structural fragments. The intense bands at 2922 and 2853 cm^{-1} are attributed to C–H stretching vibrations in the methylene groups (–CH_2–) of the glycol fragment. The signal at 1715 cm^{-1} corresponds to C=O stretching vibrations of the ester group, which is a key characteristic of the terephthalate moiety.

Peaks in the region of 1241, 1094 and 1016 cm^{-1} are associated with C–O stretching vibrations in ester and ether groups. The presence of bands at 873 and 724 cm^{-1} indicates the presence of aromatic rings (para-substituted benzene) and methylene sequences, respectively [24]. These results are consistent with the expected chemical structure of PETG, confirming the presence of both aliphatic (glycol) and aromatic (terephthalate) fragments in the polymer chain.

Figure 8 shows the FTIR spectra of PETG/PTFE-3 and PETG/PTFE-6 after testing under different loads. FTIR spectroscopy revealed that the chemical structure of PETG in all samples remained unchanged after tribological testing, as evidenced by the preservation of characteristic absorption bands at 1715 cm^{-1} (carbonyl group) and 1241 cm^{-1} (C–O bond). This is consistent with data on the structural stability of polyesters under dry sliding conditions [25].

The contact surfaces of PETG/PTFE samples with coaxially integrated PTFE exhibited clear bands characteristic of PTFE (1200, 1145 and 639 cm^{-1}), which aligns with the noticed reduction in the COF and the findings of EDS analysis. However, a broad peak in the 3600 – 3200 cm^{-1} region (hydroxyl groups) appeared in the PETG/PTFE-6 under a 100 N load, as well as in samples tested under a 150 N load. This may be due to surface oxidation occurring due to intense frictional heating. While this did not result in catastrophic failure during short-term testing, the phenomenon could adversely affect the long-term stability and service life of the material. This could potentially lead to the degradation of the polymer matrix and increased wear. For applications operating under sustained high loads, additional analysis of thermal stability and potential heat dissipation methods is required. In this study, the FTIR spectrum of the pristine PTFE insert itself remained chemically stable during testing, and no new peaks were detected.

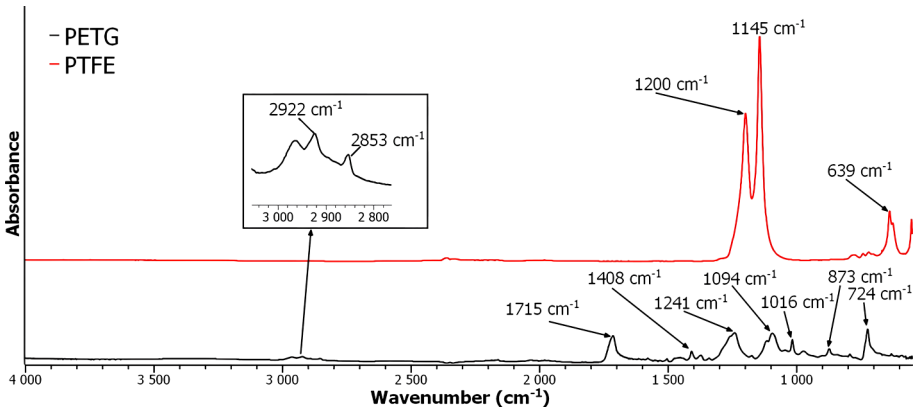

Figure 7. FTIR spectra of pristine PETG and pristine PTFE

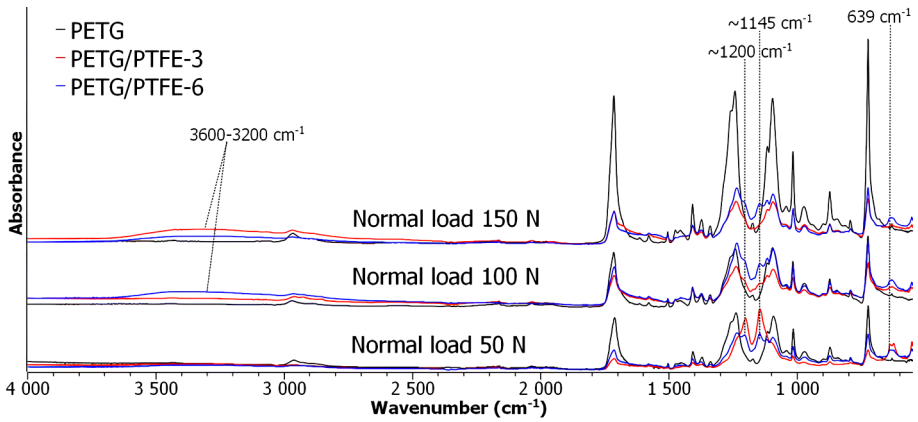

Figure 8. FTIR spectra of PETG/PTFE-3 and PETG/PTFE-6 after testing under different loads

Based on the results obtained, the following practical guideline can be proposed: for lightly to moderately loaded tribological contacts (≤ 1 MPa), a PTFE insert covering approximately 9 – 15 % of the nominal contact area is sufficient to substantially reduce the COF with minimal added complexity. For heavy-duty applications (1.5 – 2 MPa, e.g. plain bearings, linear guides and seals), an insert with a diameter providing 30 – 40 % PTFE coverage (6 mm in our geometry) is recommended to ensure low friction (0.18 – 0.24) and high wear resistance (mass loss reduced by up to 76 %).

4. Conclusion

This study demonstrates that, despite being a secondary assembly process rather than in-situ compounding, the coaxial press-fit integration of solid PTFE inserts into FDM-printed PETG parts produces a hybrid material with markedly improved tribological performance. Compared to pristine PETG, the coefficient of friction was reduced by up to 69 % and wear (measured as mass loss) by up to 76 %.

The PETG/PTFE-6 configuration exhibited the lowest steady-state coefficient of friction (between 0.18 and 0.24) and the highest wear resistance. This makes it highly promising for use in self-lubricating components, such as plain bearings and linear guides. While direct mechanical testing of the hybrid was not conducted, PETG's well-established compressive strength and rigidity suggest that the matrix retains sufficient structural integrity while the localised PTFE inserts deliver excellent anti-friction behaviour through transfer film formation.

Thermomechanical analysis confirmed the dimensional compatibility of both polymers in the 40–80 °C range. These findings provide a simple approach to manufacturing complex, self-lubricating parts that exploit the mechanical robustness of PETG and the lubrication possibilities of PTFE.

Future work could involve optimising the geometry and arrangement of multiple PTFE inserts, as well as exploring alternative polymer matrices (e.g. PA 12, PEEK or PLA) using the same integration concept. As the present study was limited to short-term testing, future research should focus on conducting long-term durability tests under various temperature and humidity conditions, as well as on combining the proposed approach with surface coatings or other solid lubricants.

References

[1] S. Singh, G. Singh, C. Prakash, S. Ramakrishna, Current status and future directions of fused filament fabrication, Journal of Manufacturing Processes, Vol. 55, 2020, pp. 288-306, DOI: 10.1016/j.jmapro.2020.04.049

[2] V. Mahesh, J.P. George, V. Mahesh, H. Chakraborthy, S. Mukunda, S.A. Ponnusami, Dry-sliding wear properties of 3D printed PETG/SCF/OMMT nanocomposites: Experimentation and model predictions using artificial neural network, Journal of Reinforced Plastics and Composites, Vol. 43, No. 11-12, 2024, pp. 682-693, DOI: 10.1177/07316844231188853

[3] E. Aslan, G. Akıncıoğlu, E. Şirin, A comparative study on friction performance and mechanical properties of printed PETG materials with different patterns, Journal of Applied Polymer Science, Vol. 142, No. 27, 2025, Paper e57136, DOI: 10.1002/app.57136

[4] O.J. Gbadeyan, T.P. Mohan, K. Kanny, Tribological properties of 3D printed polymer composites-based friction materials, in H. Jena, J.K. Katiyar, A. Patnaik (Eds.), Tribology of Polymer and Polymer Composites for Industry 4.0, Springer, Singapore, 2021, pp. 161-191, DOI: 10.1007/978-981-16-3903-6_9

[5] L.O. Vaught, A.A. Polycarpou, Investigating the effect of fused deposition modelling on the tribology of PETG thermoplastic, Wear, Vol. 524-525, 2023, Paper 204736, DOI: 10.1016/j.wear.2023.204736

[6] M.M. Hanon, R. Marczis, L. Zsidai, Impact of 3D-printing structure on the tribological properties of polymers, Industrial Lubrication and Tribology, Vol. 72, No. 6, 2020, pp. 811-818, DOI: 10.1108/ILT-05-2019-0189

[7] S. Jannet, R. Soundararajan, S.R. Kandavalli, R. Raja, Wear and friction behavior on extrusion-based 3D printed short carbon fiber reinforced PETG composites with annealing and laser treated effects, Journal of The Institution of Engineers (India): Series D, Article in Press, DOI: 10.1007/s40033-024-00794-6

[8] T. Jagadeesha, K.V. Pradeep Kumar, M.R.T. Reddy, A.J. Sankarathil, K. Raju, A.R. Junaidi, S.K. Bhat, L.C. Shashidhara, K. Revanna, N. Raghavendra, S. Udayashankar, Investigation of tribological behavior of fused deposition modelling processed parts of polyethylene terephthalate glycol polymer material, Journal of The Institution of Engineers (India): Series D, Article in Press, DOI: 10.1007/s40033-025-00885-y

[9] S.S. Bedi, V. Mallesha, Investigating tribological performance in 3D-printed PETG/graphene

composites of varying composition, Journal of Reinforced Plastics and Composites, Article in Press, DOI: 10.1177/07316844241274294

[10] V. Mahesh, Artificial neural network coupled experimental investigation of tribological behavior of additive manufactured PETG/OMMT nanocomposites, Journal of Applied Polymer Science, Vol. 140, No. 30, 2023, Paper e54089, DOI: 10.1002/app.54089

[11] M.Z. Baltić, M.R. Vasić, M.D. Vorkapić, D.M. Bajić, J. Piteľ, P. Svoboda, A. Vencl, PETG as an alternative material for the production of drone spare parts, Polymers, Vol. 16, No. 21, 2024, Paper 2976, DOI: 10.3390/polym16212976

[12] G. Gamboa, S. Mazumder, N. Hnatchuk, J.A. Catalan, D. Cortes, I. Chen, P. Perez, W. Brostow, A.B. Kaul, 3D-printed and injection molded polymer matrix composites with 2D layered materials, Journal of Vacuum Science and Technology A, Vol. 38, No. 4, 2020, Paper 042201, DOI: 10.1116/6.0000121

[13] A. Mathew, S. Ram Kishore, A.T. Tomy, M. Sugavaneswaran, S.G. Scholz, A. Elkaseer, V.H. Wilson, A. John Rajan, Vapour polishing of fused deposition modelling (FDM) parts: A critical review of different techniques, and subsequent surface finish and mechanical properties of the post-processed 3D-printed parts, Progress in Additive Manufacturing, Vol. 8, No. 6, 2023, pp. 1161-1178, DOI: 10.1007/s40964-022-00391-7

[14] T.S. Struchkova, A.P. Vasilev, A.A. Okhlopkova, S.N. Danilova, A.G. Alekseev, Mechanical and tribological properties of polytetrafluoroethylene composites modified by carbon fibers and zeolite, Lubricants, Vol. 10, No. 1, 2022, Paper 4, DOI: 10.3390/lubricants10010004

[15] N. Vidakis, M. Petousis, A. Moutsopoulou, V. Papadakis, M. Spiridaki, N. Mountakis, C. Charou, D. Tsikritzis, E. Maravelakis, Nanocomposites with optimized polytetrafluoroethylene content as a reinforcement agent in PA12 and PLA for material extrusion additive manufacturing, Polymers, Vol. 15, No. 13, 2023, Paper 2786, DOI: 10.3390/polym15132786

[16] K. Tanaka, Transfer of semicrystalline polymers sliding against a smooth steel surface, Wear, Vol. 75, No. 1, 1982, pp. 183-199, DOI: 10.1016/0043-1648(82)90147-8

[17] Z. Lin, H. Yue, B. Gao, Enhancing tribological characteristics of PEEK by using PTFE composite as a sacrificial tribofilm-generating part in a novel dual-pins-on-disk tribometer, Wear, Vol. 460-461, 2020, Paper 203472, DOI: 10.1016/j.wear.2020.203472

[18] S. Guessasma, S. Belhabib, H. Nouri, Printability and tensile performance of 3D printed polyethylene terephthalate glycol using fused deposition modelling, Polymers, Vol. 11, No. 7, 2019, Paper 1220, DOI: 10.3390/polym11071220

[19] R. Shu, R. Shen, J. Liu, Experimental investigation of the mechanical properties of PTFE scrims under high temperature conditions, Engineering Failure Analysis, Vol. 122, 2021, Paper 105222, DOI: 10.1016/j.engfailanal.2021.105222

[20] C. Yan, C. Kleiner, A. Tabigue, V. Shah, G. Sacks, D. Shah, V. DeStefano, PETG: Applications in modern medicine, Engineered Regeneration, Vol. 5, No. 1, 2024, pp. 45-55, DOI: 10.1016/j.engreg.2023.11.001

[21] T.A. Blanchet, F.E. Kennedy, Sliding wear mechanism of polytetrafluoroethylene (PTFE) and PTFE composites, Wear, Vol. 153, No. 1, 1992, pp. 229-243, DOI: 10.1016/0043-1648(92)90271-9

[22] N.K. Myshkin, M.I. Petrokovets, A.V. Kovalev, Tribology of polymers: Adhesion, friction, wear, and mass-transfer, Tribology International, Vol. 38, No. 11-12, 2006, pp. 910-921, DOI: 10.1016/j.triboint.2005.07.016

[23] P. Samyn, G. Schoukens, Experimental extrapolation model for friction and wear of polymers on different testing scales, International Journal of Mechanical Sciences, Vol. 50, No. 9, 2008, pp. 1390-1403, DOI: 10.1016/j.ijmecsci.2008.07.002

[24] A.S. Lenshin, V.E. Frolova, S.S. Ivkov, E.P. Domashevskaya, Microstructural and hydrophilic properties of polyethylene terephthalate glycol polymer samples with different 3D printing patterns, Condensed Matter and Interphases, Vol. 26, No. 1, 2024, pp. 78-87, DOI: 10.17308/kcmf.2024.26/11810

[25] Z. Zuo, L. Song, Y. Yang, Tribological behavior of polyethersulfone-reinforced polytetrafluoroethylene composite under dry sliding condition, Tribology International, Vol. 86, 2015, pp. 17-27, DOI: 10.1016/j.triboint.2015.01.019